ORIGINAL RESEARCH ARTICLE

# Carotid arterial mechanics as useful biomarker of extracellular matrix turnover and preserved ejection fraction heart failure

Kevin Ning Zhou[1], Kuo-Tzu Sung[2,3,5], Chih-Hsuan Yen[2,3,4,5], Cheng-Huang Su[2,3,5], Ping-Ying Lee[2,3,5], Ta-Chuan Hung[2,3,5], Wen-Hung Huang[2,3,4,5], Shih-Chieh Chien[6], Jui-Peng Tsai[2,3,5,7], Chun-Ho Yun[7,8], Shun-Chuan Chang[2], Hung-I Yeh[2,4] and Chung-Lieh Hung[2,3,5,9]*

[1]*Williams College Department of Biology, Williams College, 59 Lab Campus Drive, Williamstown, MA 01267, USA;* [2]*Department of Medicine, Mackay Medical College, New Taipei City, Taiwan;* [3]*Mackay Junior College of Medicine, Nursing, and Management, Taipei, Taiwan;* [4]*Institute of Preventive Medicine, School of Public Health, National Taiwan University, Taipei, Taiwan;* [5]*Cardiovascular Division, Department of Internal Medicine, MacKay Memorial Hospital, Zhongshan North Road, Taipei, 104, Taiwan;* [6]*Department of Critical Care Medicine, MacKay Memorial Hospital, Taipei, Taiwan;* [7]*Department of Biomedical Imaging and Radiological Sciences, National Yang Ming University, Taipei, Taiwan;* [8]*Department of Radiology, MacKay Memorial Hospital, Taipei, Taiwan;* [9]*Institute of biomedical sciences, Mackay Medical College, New Taipei City, Taiwan*

## Abstract

**Aims** We aimed to investigate the functional alterations, diagnostic utilization, and prognostic implication of carotid arterial deformations in subjects with cardiovascular risk factors and heart failure (HF) with preserved ejection fraction (HFpEF).
**Methods and results** Among 251 prospectively participants (mean age 66.0 ± 9.8 years, 65.7% female) in a single centre between December 2011 and September 2014, carotid artery deformations including circumferential strain (CCS)/strain rate and radial strain were analysed by two-dimensional speckle tracking. We further related these carotid artery deformation indices to HF biomarkers and cardiac structure and function by echocardiography and explored their prognostic values. Significant reductions of CCS, circumferential strain rate, and circumferential radial strain were observed across control ($n$ = 52), high risk ($n$ = 147), and HFpEF ($n$ = 52) (trend $P \leq 0.001$). Aging, hypertension, HFpEF, and higher pulse rate showed independent associations with reduced CCS by stepwise multivariate regressions (all $P < 0.05$). Higher CCS was inversely associated with better cardiac remodelling and functional indices, and lower multiple HF biomarkers (all $P \leq 0.005$). After adjustment, higher CCS was independently associated with better global ventricular longitudinal strain/early diastolic strain rate, lower matrix metalloproteinase-2, and N-terminal propeptide of procollagen type III levels (adjusted coef: −0.08 and −19.9, all $P < 0.05$). During a median follow-up of 1406 days (interquartile range: 1342–1720 days), CCS less than 3.28% as a cut-off had markedly higher HF events [Harrell's C: 0.72, adjusted HR: 2.20 (95% confidence interval: 1.24, 3.16), $P$ = 0.008]. CCS also showed significantly improved risk prediction for HF over global ventricular longitudinal strain (net reclassification index: 48%, $P$ = 0.001; integrated discrimination improvement: 1.8%, $P < 0.001$).
**Conclusions** Carotid artery deformations using two-dimensional speckle-tracking imaging showed novel mechanistic insights on functional arterial alterations reflecting coupled arterial-ventricular pathophysiology. Utilization of such measure may further provide additive prognostic value to advanced myocardial functional assessment.

# Introduction

Heart failure (HF) remains a global epidemic, affecting >30 million individuals. A significant proportion of elderly patients is present with HF with preserved ejection fraction (HFpEF).[1,2] With the rapid rise in global life expectancy and the increasing prevalence of comorbidities, HFpEF has emerged as a rapidly growing public health concern worldwide.[3,4] Although several echocardiographic parameters, such as geometric remodelling, haemodynamic alterations, and myocardial diastolic indices, have been proposed as indicators of HFpEF, these markers are neither sensitive nor specific.[4–7] Central arterial remodelling and altered vascular mechanical properties have been proposed as critical components of HFpEF pathophysiology in the elderly and hypertensive population[8,9], although it remains largely underused in daily clinical practices during diagnosis or risk stratification.

Reduced elasticity and increased arterial stiffness remain as the earliest manifestations within vascular wall pathology among aging and hypertensive patients.[8–11] Shared pathophysiology of excessive extracellular matrix turnover and elastic fibre breakdown in the vascular wall and myocardial tissue may likely occur during aging and hypertension (HTN), leading to unfavourable left ventricular (LV)-arterial coupling, decreased compliance, and HFpEF development.[6–9,12] Limited buffering capacity from reduced arterial compliance may cause excessive stress load on the ventricles during ejection, which adds excessive and detrimental burden on the myocardial tissue.[10] Currently, there is controversy regarding conventional parameters for precisely quantifying local arterial stiffness.[13] Two-dimensional (2D) speckle-tracking for functional cardiovascular strain measure can be angle independent with less variability; it has been deemed as a novel approach and a more specific approach for quantifying both subclinical myocardial and arterial dysfunctions with validity, especially in HTN.[14–17] However, the discriminative ability and prognostic utilization of vascular strain in HFpEF patients remains largely unexplored.[13,18]

Therefore, this study aimed to compare carotid deformations with established cardiac functional indices as markers of pathological maladaptive LV-arterial processes coupled to subclinical ventricular dysfunction. We further sought to investigate the diagnostic yield of mechanical carotid vascular deformations and potential prognostic implications in HFpEF patients or those at a high risk of HFpEF development.

# Methods

## Study population

For this prospectively conducted analysis, 261 study participants were enrolled from outpatient clinics at Mackay Memorial Hospital in Taipei, Taiwan, between December 2011 and September 2014. Written informed consent was obtained from all patients, and the study was approved by the institutional review board of the Mackay Memorial Hospital (approval numbers: 11MMHIS127 and 15MMHIS031e). The aim of current study was to assess the impacts of potential cardiometabolic factors on cardiovascular manifestations, including cardiac structural/functional alterations and vascular mechanical characteristics. Patients with atrial fibrillation, moderate-to-severe valvular heart disease, and prior hospitalization for systolic HF were excluded. Study participants were categorized into three groups: (i) healthy control group (*n* = 53) comprising those underwent annual health survey without known cardiovascular risk factors or systemic diseases who volunteered to participate in this study; (ii) high-risk group (*n* = 154), including patients enrolled from outpatient clinics without prevalent HF or known HF history who carried at least one cardiometabolic risk, such as HTN, diabetes mellitus (DM), dyslipidaemia, obesity [>Grade 1, body mass index (BMI) ≥ 30 kg/m$^2$], or central obesity: waist circumference>90 cm (male) or>80 cm (female); and (iii) HFpEF group (*n* = 54), which included patients who had known prior HF hospitalization history with an ejection fraction of 50% or higher. We prospectively followed the study participants for at least 3 years after study enrolment with a pre-specified endpoint of incident HF. The main inclusion and exclusion criteria for the study are displayed in Supporting Information, *Figure S1*.

The presence of a history of HTN was defined as systolic blood pressure > 140 mmHg, diastolic blood pressure > 90 mmHg, or previous diagnosis of HTN under pharmaceutical control. DM was defined as fasting blood glucose level > 126 mg/dL or previous diagnosis of DM under pharmaceutical control. Dyslipidaemia was defined by elevated levels of low-density lipoprotein cholesterol and total cholesterol, or abnormal levels of high-density lipoprotein cholesterol before the usage of anti-lipid drugs, such as statins or fibrates. Cardiovascular disease (CVD) was defined by a prior history of myocardial infarction, coronary artery post angioplasty, or history of cerebrovascular events.

## Conventional echocardiography, carotid sonography, and two-dimensional speckle-tracking protocol

Vascular strain analysis was performed on both sides of the carotid arteries using an offline work station equipped with grey-scale (2D), B-mode EchoPac speckle-tracking software (GE Vingmed Ultrasound) (*Figure 1A*). After selecting the sequence with the least motion artefacts, the technician marked a 'region of interest' (ROI) by placing marking indicator points in the intima-media complex. The software then used these marking points to calculate the circumferential

**Figure 1** (A) Tracing carotid artery kinetics and deformational indices from arterial wall of B-mode image, and (B) automatic tracking with six different regions. Curves of carotid circumferential strain (CCS) (C) and strain rate (CCSR) (D) from tracking were displayed.
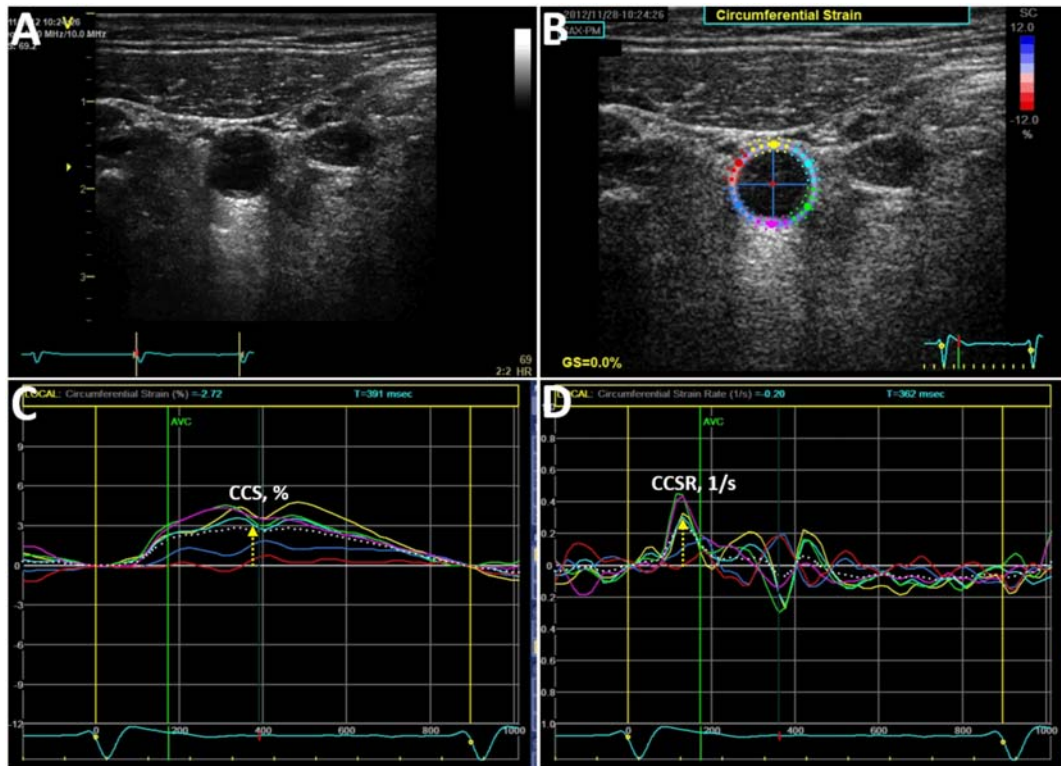


contour of the vessel. The initial ROI width was 1.6 mm and was adjusted to match the width of the arterial wall. ROI width and boundaries were checked by eye and then verified by the machine. 'Global' values for the entire ROI were assessed. Adequate speckle-tracking-based analysis was verified by the operator and adjusted if necessary. The software automatically divided the vessel wall into six regions and assessed local parameters. Adequate tracking for all six segments was verified (Supporting Information, *Figure S2A*), and, if necessary, the ROI was recalculated after minor manual adjustment for the vascular edges (*Figure 1B*). Cardiac deformations of global ventricular longitudinal strain (GLS) and global circumferential strain (GCS) were averaged from peak strains from three apical views (four-chamber, two-chamber, and three-chamber views for GLS) and short-axis layers (mitral, papillary muscle, and apical layers for GCS) as our previous publication, with systolic (SRs), early (SRe), and late diastolic strain rate components obtained using same software.[18] In addition to deformation measures, conventional echocardiography was performed using a 2.5 MHz transducer, with structural and functional parameters including LV wall thickness, internal diameter, LV mass (with and without index), early mitral inflow E and tissue Doppler determined (TDI) myocardial systolic (TDI-s'), and early diastolic velocity (TDI-e') obtained (averaged from both septal and lateral walls). LV filling was estimated using E divided by TDI-e' (E/TDI-e').

Carotid arterial characterization and deformation measures using grey-scale, B-mode speckle-tracking have been well validated via *in vitro* sonomicrometry[19] and applanation tonometry[20] in previous work; carotid circumferential strain (CCS), circumferential strain rate (CCSR), radial strain (CRS), and displacement (CRD) (Supporting Information, *Figure S2B* and *S2C*) were all analysed using algorithms of previous studies (by K. N. Z.) blinded to clinical information. [13,21] During systole, the CCS assumes positive values due to stretching or expansion of the CRS (%); conversely, CRS becomes negative as a result of vessel wall compression.[22] CRD values (mm) were obtained and averaged for both sides of the carotid vessel wall. The B-mode dynamic images from short-axis carotid artery motions over all cardiac cycles for three continuous beats were recorded. Peak values for CCSR, CRS, and CRD across the six segments were averaged and recorded from both sides of carotid arteries, with mean value as the representative estimates of each study participant, as established previously.[13] Maximal intima-media thickness (IMT) of the common carotid artery was defined as the mean of the maximal IMT of the near and far wall on both the left and right sides (95% available for both sides). Carotid artery diameter was measured between the two leading edges of the near-wall and far-wall intima at the same site as the IMT measurement at the end-diastolic phase using electrocardiogram-gated imaging.[14]

## Follow-up and outcomes determination

We pre-specified the primary outcome as incident HF events. Incident HF events were defined by clinical HF signs/symptoms requiring urgent and unplanned hospitalization or emergency department visit requiring intravenous diuretic or vasodilator treatment, or new or worsening HF with evidenced pulmonary congestion/oedema requiring admission adjudicated by cardiologists following the study index date. The secondary outcome was composite HF and all-cause mortality (whichever came first) following the study index date, with any study subjects without any outcome censored at the date of last follow-up during observation.

**Table 1** Baseline demographic characteristics, biomarkers, echocardiography, and carotid vascular ultrasonography information of study participants

| | Control | High risk | HFpEF | *P*-value (ANOVA/$X^2$) | *P*-value (trend) |
|---|---|---|---|---|---|
| Total (*n* = 251) | (*n* = 52) | (*n* = 147) | (*n* = 52) | | |
| **Demographics** | | | | | |
| Age, years | 60.0 ± 6.3 | 66.3 ± 9.7* | 72.0 ± 9.4*,† | <0.001 | <0.001 |
| Sex (female) (%) | 64.2 | 60.1 | 80 | 0.024 | 0.08 |
| BMI (kg/m$^2$) | 23.0 ± 2.9 | 27.4 ± 4.1* | 28.0 ± 5.2* | <0.001 | <0.001 |
| Systolic blood pressure (mmHg) | 128.4 ± 17.2 | 141.9 ± 18.7* | 146.9 ± 20.5* | <0.001 | <0.001 |
| Diastolic blood pressure (mmHg) | 77.7 ± 11.2 | 81.6 ± 12.1 | 80.8 ± 13.1 | 0.13 | 0.19 |
| Heart rate (b.p.m.) | 72.6 ± 9.24 | 76.7 ± 11.9 | 76.6 ± 10.8 | 0.06 | 0.07 |
| **Laboratory data** | | | | | |
| Fasting glucose (mg/dL) | 95.4 ± 9.47 | 112.5 ± 30.9* | 137.1 ± 57.9*,† | <0.001 | <0.001 |
| Cholesterol (mg/dL) | 209.5 ± 43.0 | 198.4 ± 42.1 | 189.2 ± 43.0 | 0.08 | 0.067 |
| HDL-C (mg/dL) | 64.1 ± 16.9 | 53.1 ± 18.5* | 50.0 ± 19.2* | <0.001 | <0.001 |
| Uric acid (mg/dL) | 5.2 ± 1.0 | 5.9 ± 1.4 | 6.7 ± 1.8 | <0.001 | <0.001 |
| eGFR (mL/min/1.73 m$^2$) | 92.0 ± 16.2 | 78.0 ± 25.0* | 67.8 ± 29.4*,† | <0.001 | <0.001 |
| **Biomarkers** | | | | | |
| hs-CRP (median, 25th75th) (mg/dL) | 0.073 (0.0390.135) | 0.13 (0.0610.31)* | 0.23 (0.080.48)*,† | <0.001 | <0.001 |
| BNP (median, 25th75th) (pg/mL) | 5 (517.8) | 20 (846)* | 106 (44249)*,† | <0.001 | <0.001 |
| PIIINP (median, 25th75th) (U/mL) | 0.67 (0.5850.78) | 0.94 (0.7451.165)* | 1.14 (0.991.47)*,† | <0.001 | <0.001 |
| Galectin-3 (median, 25th-75th) (ng/mL) | 1.36 (0.672.41) | 2.365 (1.433.39)* | 2.85 (1.955.79)*,† | <0.001 | <0.001 |
| MMP-2 (ng/mL) | 215.8 ± 48.4 | 230.7 ± 70.3 | 250.6 ± 95.1* | 0.022 | 0.007 |
| **Medical history** | | | | | |
| Hypertension (%) | 0 | 88.9 | 94.6 | <0.001 | <0.001 |
| Diabetes mellitus (%) | 0 | 31.4 | 58.9 | <0.001 | <0.001 |
| Hyperlipidaemia (%) | 0 | 54.0 | 64.3 | <0.001 | <0.001 |
| Cardiovascular disease (%) | 0 | 17.0 | 31.4 | <0.001 | <0.001 |
| **Echocardiography parameters** | | | | | |
| Septal wall thickness (mm) | 8.28 ± 0.96 | 9.21 ± 1.29* | 10.2 ± 1.71*† | <0.001 | <0.001 |
| LV internal diameter (mm) | 44.7 ± 3.79 | 46.7 ± 3.36* | 46.3 ± 4.83 | 0.006 | 0.04 |
| RWT | 0.37 ± 0.04 | 0.40 ± 0.05* | 0.43 ± 0.07*,† | <0.001 | <0.001 |
| LV mass index (g/m$^2$) | 70.1 ± 18.6 | 78.9 ± 16.5* | 90.2 ± 20.8*,† | <0.001 | <0.001 |
| TDI-e′ (average) (cm/s) | 8.87 ± 1.70 | 7.76 ± 1.86* | 6.45 ± 1.56*,† | <0.001 | <0.001 |
| TDI-s′ (average) (cm/s) | 7.94 ± 1.34 | 7.81 ± 1.36 | 6.72 ± 1.39*,† | <0.001 | <0.001 |
| E/TDI-e′ (average) | 7.45 ± 1.85 | 9.46 ± 2.89* | 13.3 ± 4.3*,† | <0.001 | <0.001 |
| GCS (%) | −21.2 ± 2.44 | −20.7 ± 2.76 | −20.1 ± 3.42 | 0.17 | 0.061 |
| GLS (%) | −20.9 ± 2.07 | −19.9 ± 1.95* | −17.1 ± 2.75*,† | <0.001 | <0.001 |
| LV SRs (average) (1/s) | −1.22 ± 0.14 | −1.11 ± 0.15* | −1.04 ± 0.17*,† | <0.001 | <0.001 |
| LV SRe (average) (1/s) | 1.24 ± 0.32 | 1.08 ± 0.27* | 0.97 ± 0.29*,† | <0.001 | <0.001 |
| LV SRa (average) (1/s) | 1.17 ± 0.21 | 1.20 ± 0.23 | 1.13 ± 0.31 | 0.17 | 0.38 |
| **Vascular carotid arterial indices** | | | | | |
| IMT (mm) | 0.84 ± 0.13 | 0.86 ± 0.14 | 1.01 ± 0.16*,† | <0.001 | <0.001 |
| Circumferential strain (CCS) (%) | 4.15 ± 0.66 | 3.70 ± 0.52* | 3.40 ± 0.42*,† | <0.001 | <0.001 |
| Circumferential strain rate (CCSR) (1/s) | 0.49 ± 0.14 | 0.45 ± 0.13* | 0.38 ± 0.11* | 0.001 | <0.001 |
| Radial strain (CRS) (%) | −3.37 ± 1.08 | −3.01 ± 1.03 | −2.83 ± 1.05* | 0.037 | 0.013 |
| Radial displacement (CRD) (mm) | −0.29 ± 0.12 | −0.27 ± 0.11 | −0.26 ± 0.07 | 0.17 | 0.08 |

ANOVA, analysis of variance; BMI, body mass index; BNP, brain natriuretic peptide; ED, end-diastole; eGFR, estimated glomerular filtration rate; GCS, global circumferential strain; GLS, global longitudinal strain; HDL-C, high-density lipoprotein cholesterol; HFpEF, heart failure with preserved ejection fraction; hs-CRP, high-sensitivity C-reactive protein; IMT, intima-media thickness; LV, left ventricular; MMP-2, matrix metalloproteinase-2; PI, pulsatility index; PIIINP, N-terminal propeptide of procollagen type III; PS, pulmonary stenosis; RI, resistance index; RWT, relative wall thickness; SR, systolic rate; SRa, late diastolic strain rate; SRe, early diastolic strain rate; TDI-e′, myocardial relaxation velocity; TDI-s′, myocardial contraction velocity.
*ANOVA *P* < 0.05 vs. non-hypertension.
#ANOVA *P* < 0.05 vs. hypertension.
†ANOVA *P* < 0.05 vs. HFpEF.
¥Spearman *P* < 0.0001.

## Statistical analyses

The test for normal distribution (Skewness Kurtosis test) was assessed before descriptive and inference analyses. For normally distributed continuous variables, data were presented as mean ± standard deviation, or as median and interquartile range for non-normally distributed variables. Comparisons of continuous variables among different clinical disease categories (as healthy control, high-risk, and HFpEF groups) were performed by one-way analysis of variance (one-way ANOVA) with post hoc pairwise comparisons (*Table 1*), with categorical variables were presented by percentage or proportional ratios and further compared by the chi-squared statistic or Fisher's exact test, as appropriate. Correlations between clinical disease categories and demographics, laboratory data, medical histories, echocardiography parameters, and carotid deformations (i.e. CCS and CCSR) were evaluated using

Pearson's correlation coefficient and linear regression model (*Table 2*). Multivariate backward stepwise linear regression models between carotid deformation measures (i.e. CCS and CCSR) and key clinical covariates [with coefficient values and 95% confidence intervals (CIs) reported] were constructed to establish the determinants of carotid deformation measures; variables with $P > 0.10$ were removed from model (Supporting Information, *Table S1*).

The prognostic implication of carotid deformations on clinical outcomes of incident HF/death events were explored using Cox proportional hazards model. Potential confounders entered into multivariate Cox regression models were based on clinical considerations for HFpEF risk factors including age, sex, BMI, systolic blood pressure, medical history of HTN, DM, and CVD, and renal function in terms of estimated glomerular filtration rate (*Table 3*). Differences in various carotid artery sonography indices between subjects with and

**Table 2** Associations of circumferential strain and strain rate with biomarkers and echocardiography information

| | Circumferential strain (CCS) (%) | | | Circumferential strain rate (CCSR) (1/s) | | |
|---|---|---|---|---|---|---|
| | Pearson's correlation | Coef. (95% CI) | P-value | Pearson's correlation | Coef. (95% CI) | P-value |
| Biomarkers | | | | | | |
| hs-CRP (+1 mg/dL) | −0.18 | −0.34 (−0.58, −0.09) | 0.007 | −0.14 | −0.05 (−0.11, 0.003) | 0.06 |
| BNP (+100 pg/mL) | −0.23 | −0.11 (−0.18, −0.05) | <0.001 | −0.17 | −0.02 (−0.03, −0.004) | 0.014 |
| PIIINP (+1 U/mL) | −0.35 | −0.55 (−0.74, −0.36) | <0.001 | −0.25 | −0.08 (−0.13, −0.04) | <0.001 |
| Galectin-3 (+1 ng/mL) | −0.19 | −0.05 (−0.08, −0.02) | 0.004 | −0.15 | −0.008 (−0.01, −0.001) | 0.033 |
| MMP-2 (+100 ng/mL) | −0.15 | −0.13 (−0.23, −0.03) | 0.012 | 0.04 | 0.01 (−0.02, 0.03) | 0.62 |
| Echocardiography parameters | | | | | | |
| LV mass index (g/m$^2$) | −0.17 | −0.006 (−0.01, −0.001) | 0.009 | −0.19 | −0.001 (−0.002, −0.0003) | 0.008 |
| TDI-e' (average) (cm/s) | 0.33 | 0.11 (0.07, 0.15) | <0.001 | 0.27 | 0.02 (0.01, 0.03) | <0.001 |
| TDI-s' (average) (cm/s) | 0.13 | 0.06 (0.002, 0.11) | 0.043 | 0.18 | 0.02 (0.004, 0.03) | 0.009 |
| E/TDI-e' (average) | −0.29 | −0.05 (−0.08, −0.03) | <0.001 | −0.18 | −0.01 (−0.01, −0.002) | 0.008 |
| GCS (%) | −0.18 | −0.05 (−0.08, −0.02) | 0.001 | −0.11 | −0.006 (−0.012, 0.001) | 0.07 |
| GLS (%) | −0.35 | −0.08 (−0.10, −0.05) | <0.001 | −0.26 | −0.01 (−0.02, −0.008) | <0.001 |
| LV SRs (average) (1/s) | −0.27 | −1.09 (−1.58, −0.60) | <0.001 | −0.28 | −0.24 (−0.35, −0.13) | <0.001 |
| LV SRe (average) (1/s) | 0.44 | 0.90 (0.66, 1.13) | <0.001 | 0.33 | 0.15 (0.10, 0.20) | <0.001 |
| LV SRa (average) (1/s) | −0.11 | −0.29 (−0.60, 0.03) | 0.07 | −0.11 | −0.06 (−0.13, 0.02) | 0.11 |
| IMT (mm) | −0.24 | −0.91 (−1.37, −0.44) | <0.001 | −0.16 | −0.14 (−0.25, −0.03) | 0.013 |

BNP, brain natriuretic peptide; CI, confidence interval; Coef., coefficient; GCS, global circumferential strain; GLS, global longitudinal strain; hs-CRP, high-sensitivity C-reactive protein; IMT, intima-media thickness; LV, left ventricular; MMP-2, matrix metalloproteinase-2; PIIINP, N-terminal propeptide of procollagen type III; RWT, relative wall thickness; SR, systolic rate; SRa, late diastolic strain rate; SRe, early diastolic strain rate; TDI-e, myocardial relaxation velocity; TDI-s', myocardial contraction velocity.

**Table 3** Associations of carotid arterial deformation and sonography indices with clinical end points

| | HF/death events (−) (n = 180) | HF/death events (+) (n = 67) | P-value | Harrell's C-index | HR (adjusted) (95% CI) | P-value |
|---|---|---|---|---|---|---|
| IMT (mm) | 0.85 ± 0.14 | 0.97 ± 0.18 | <0.001 | 0.66 | 3.16 (0.53, 18.9) | 0.21 |
| Carotid circumferential strain (CCS) (%) | 3.85 ± 0.59 | 3.39 ± 0.43 | <0.001 | 0.72 | 0.47 (0.25, 0.89) | 0.02 |
| Carotid circumferential strain rate (CCSR) (1/s) | 0.46 ± 0.14 | 0.37 ± 0.09 | <0.001 | 0.68 | 0.05 (0.005, 0.62) | 0.019 |
| Carotid radial strain (CRS) (%) | −3.11 ± 1.08 | −2.87 ± 0.97 | 0.14 | 0.55 | 1.21 (0.93, 1.56) | 0.15 |
| Carotid radial displacement (CRD) (mm) | −0.28 ± 0.11 | −0.25 ± 0.07 | 0.09 | 0.54 | 5.87 (0.21, 167.3) | 0.30 |

CI, confidence interval; HF, heart failure; HR, hazard ratio. Other abbreviations as *Table 1*.
Models were adjusted for age, sex, body mass index, systolic blood pressure, medical history of hypertension, diabetes, and cardiovascular diseases and renal function in terms of estimated glomerular filtration rate (eGFR).

without incident HF/death events were further compared using the unpaired *t*-test (*Table 3*). By using a time-dependent receiver-operator characteristic curve method for HF events (Harrell's C-statistics), we defined the optimal cut-offs for various carotid artery deformation indices, with C-statistics reported as a measure of prediction accuracy of HF-related events (*Figure 2A*). Kaplan–Meier survival curves were constructed and compared by choosing optimal CCS cut-off value ($<$, $\geq$3.28%, respectively, with CCS $<$ 3.28% defined as abnormal CCS) using the log-rank test under assumptions of proportional hazard rates (*Figure 3B*). Incremental prognostic performance with CCS was

assessed using the net reclassification improvement and integrated discrimination improvement indices.

Statistical significance was set at two-sided $P < 0.05$. Owing to the multiple associations found between carotid deformations, cardiac echocardiography parameters and circulating biomarkers, multiple hypothesis testing was corrected by Bonferroni method with statistical significance set at $P < 0.01$ (0.05 divided by 10, $P < 5*10^{-3}$). SPSS software version 17.0 statistical software (SPSS, Chicago, IL, USA), STATA software (version 11.0, Stata-Corp., College Station, TX, USA), and R version 3.2.5 were used for all statistical analyses.

**Figure 2** (A) Side by side box plot showing the values and ranges of CCS across categories of healthy control (control, n = 52), hypertension (HTN, n = 130), and HFpEF groups (n = 52). [†]$P < 0.05$ compared with healthy, [¥]$P < 0.05$ compared with HTN group; (B) scatterplot correlation between CCS and GLS. The red dotted line indicates the boundary for impaired global LV systolic strain GLS ($> -18$%); (C) distribution of prevalent HFpEF according to the CCS tertiles. (D) Restricted cubic spline (RCS) analysis showing the unadjusted hazard ratio (red line) and 95% confidence lower and upper limits (dark blue lines) for the clinical endpoint of HF admission (n = 61; reference value: 3.28%). CCS, carotid circumferential strain; GLS, global longitudinal strain; HF, heart failure; HFpEF, heart failure with preserved ejection fraction; LV, left ventricular.
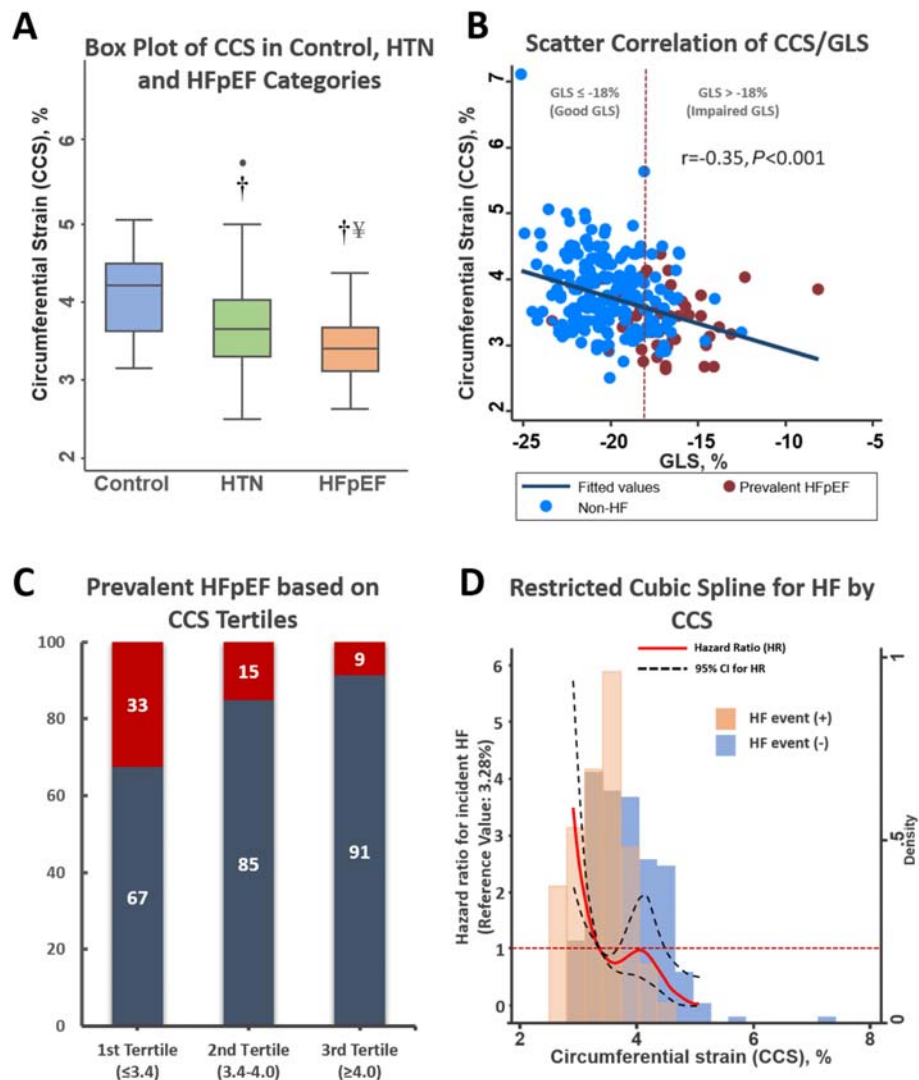
**Figure 3** (A) CCS, CCSR, CRS, and CRD in non-HF and HF patients; (B) Kaplan–Meier survival curves for CCS at a cut-off value of 3.28%; (C) composite HF admission/death events during follow-up defined by impaired global GLS ($>, \leq -18\%$). CCS, carotid circumferential strain; CCSR, carotid circumferential strain rate; CRS, carotid radial strain; CRD, carotid radial displacement; GLS, global longitudinal strain; HF, heart failure; HFpEF, heart failure with preserved ejection fraction.
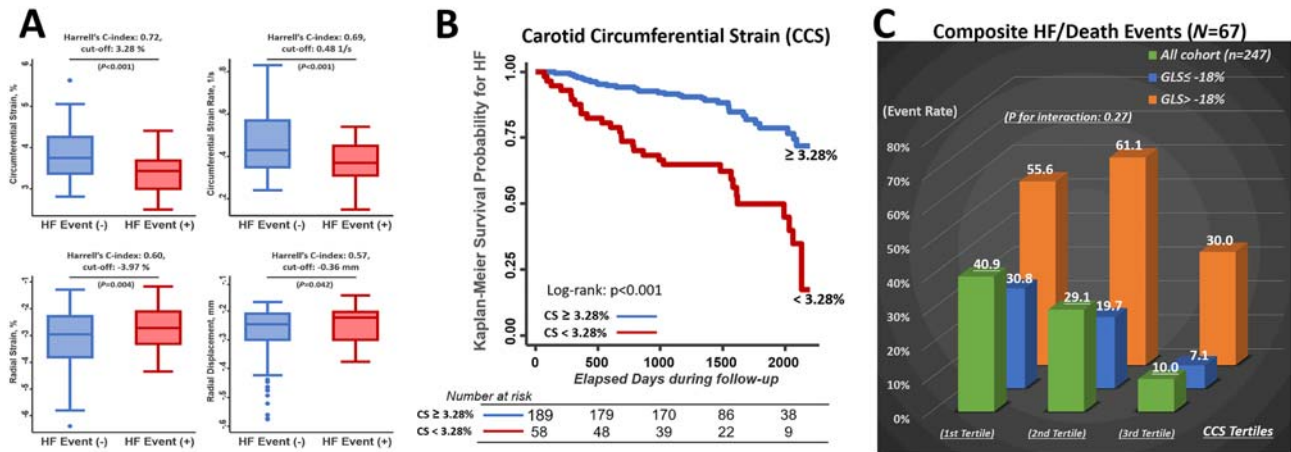


# Results

## Baseline demographic information, echocardiography, and carotid deformation indices

Totally 251 subjects had sufficient carotid arterial deformation measures available after exclusion (Table 1). Subjects in the high-risk/obesity or HFpEF groups tended to be older, were more likely to be women, had higher BMIs, higher blood pressure, showed more unfavourable lipid profiles, had worse renal functions, showed higher levels of brain natriuretic peptide, N-terminal propeptide of procollagen type III (PIIINP) and galectin-3, and were more likely to have cardiac comorbidities including HTN, DM, hyperlipidaemia, and CVD (all $P < 0.05$). A greater extent of cardiac remodelling, more impaired LV diastolic functional indices, reduced myocardial contractility velocity (TDI-s′), worsened systolic longitudinal strain (GLS), and SRs/SRe were observed in these subjects (all $P < 0.001$).

The mean values of CCS, CCSR, CRS, and CRD were $3.73 \pm 0.58$, $0.43 \pm 0.13$, $-3.05 \pm 1.06$, and $-0.27 \pm 0.10$, respectively. A significant and graded reduction of mean CCS values across the control, high-risk, and HFpEF disease groups were observed (Table 1) ($4.15 \pm 0.66\%$, $3.70 \pm 0.51\%$, and $3.39 \pm 0.42\%$, respectively; ANOVA $P < 0.001$). Histograms of CCS, CCSR, CRS, and CRD were displayed in Supporting Information, Figure S3. Compared with the non-HFpEF (control and high-risk groups), HFpEF showed significantly lower baseline CCS and CCSR (Supporting Information, Figure S4). When study participants were alternatively divided into control ($n = 52$), HTN ($n = 130$), and HFpEF groups ($n = 52$), there were consistent functional declines in both CCS and CCSR (both $P < 0.001$) (Figure 2A).

## Reproducibility of carotid deformation indices

A random sample of 34 subjects in the current study was chosen to assess the reproducibility in our lab, the inter-observer variability of CCS, CCSR, and CRS based on coefficients of variance of 4.64%, 6.77%, 7.44%, and 9.8%; the intra-observer variability was 3.59%, 5.06%, 5.4%, and 8.2%, respectively.

## Associations of carotid deformation indices with biomarkers and cardiac structure and function

Higher CCS was inversely associated with lower circulating pro-inflammatory and HF biomarkers, including high sensitivity C-reactive protein, brain natriuretic peptide, PIIINP, and galectin-3 (all $P \leq 0.005$), and borderline lower extracellular turnover marker of matrix metalloproteinase-2 (MMP-2) ($P = 0.012$). Higher CCS was also associated with lesser degree of LV remodelling, higher TDI-e′/TDI-s′, lower E/TDI-e′ and better LV deformations of GLS (Figure 2A, $r = -0.35$, $P < 0.001$), GCS, and longitudinal strain rates of SRs/SRe (Table 2, all $P < 0.005$), but not with LVEF ($P = $ NS). Sex-stratified analysis revealed borderline more pronounced associations of CCS with LV GCS and PIIINP (both $P_{\text{interaction}}$: 0.06) (Supporting Information, Figure S5). After adjustment, higher CCS was independently associated with better GLS [adjusted coef. $-0.92$ ($-1.43$, $-0.41$), $P < 0.001$] better myocardial relaxation LV SRe [adjusted coef. $-0.12$ ($-0.18$, $-0.06$), $P < 0.001$], and lower PIIINP and MMP-2 levels [adjusted coef. $-0.08$ ($-0.16$, $-0.004$), $P = 0.038$; $-19.9$ ($-37.6$, $-2.16$), $P = 0.028$, respectively]. Similar though attenuated relations were observed with CCSR (Table 2), with CRS and

CRD showed less significant associations (Supporting Information, *Table S2*). A significantly lower proportion of abnormal GLS ($> -18.0\%$) (40.5%, 22.8%, and 10.0%) along with lower prevalent HFpEF (33%, 15%, and 9%) were observed across greater CCS tertiles (1st: $\leq 3.4\%$; 2nd: 3.4%–4.0%; and 3rd: $\geq 4.0\%$) (*Figure 2B*). Compared with preserved GLS ($\leq -18.0\%$), those with impaired GLS ($> -18.0\%$) showed markedly worse CCS (3.46% vs. 3.82%, $P < 0.001$).

## Outcomes

During a median follow-up of 1406 days (interquartile range: 1342–1720 days), 4 (three from control and one from high-risk groups) out of 251 study participants were lost to follow-up (loss to follow-up rate: 1.6%). Of the remaining 247 participants with follow-up, 61 (24.7%) participants experienced HF events, and 11 had all-cause mortality events, with 67 (27.1%) had composite HF/mortality events. Lower CCS appeared to be associated with higher incident HF admission in a nonlinear relationship (*Figure 2C*). Both CCS and CCSR yielded good prediction accuracy for HF admission events (*Figure 3A*, Harrell's C-statistics: 0.72 and 0.69 for CCS and CCSR, respectively). In fully adjusted models, higher CCS and CCSR conferred better prognostic values for HF [adjusted hazard ratio (HR): 0.36 (95% CI: 0.18, 0.72) and 0.03 (95% CI: 0.002, 0.40), $P = 0.004$ and 0.008, respectively] and composite HF admission and all-cause death [adjusted HR: 0.47 (95% CI: 0.25, 0.89) and 0.05 (95% CI: 0.005, 0.62), $P = 0.02$ and 0.019, respectively] among various carotid Doppler ultrasonic parameters (*Table 3*). By choosing optimal cut-off value ($< 3.28\%$), abnormal CCS was well discriminated and was associated with a doubled risk for incident HF even after adjustment [*Figure 3B*, adjusted HR: 2.20 (95% CI: 1.24, 3.16), $P = 0.008$]. Overall, graded reduction of HF and death events were observed across greater CCS tertile groups, with subjects categorized into lower (first and second tertiles) CCS tertiles and abnormal ventricular strain (GLS $> -18\%$), demonstrating the highest rates of clinical HF and death (*Figure 3C*) ($P_{\text{interaction}}$ for effects of CCS tertiles modifying abnormal GLS in HF/death: 0.27). The superiority of incremental values of CCS over cardiac contractility indices on patient classification for HF were significantly improved when CCS was added to the global LV contractility index of GLS (category-free, continuous net reclassification improvement: 48%; $P = 0.001$; integrated discrimination improvement: 1.8%, $P < 0.001$) (Supporting Information, *Table S3*) with the same adjustments for covariates.

## Discussion

Our main findings are three-fold: (i) significant and graded reduction of speckle-tracking-based carotid artery deformations including CCS/CCSR were observed across healthy, high-risk, and HFpEF patients; (ii) mechanical carotid artery properties using 2D deformation indices were tightly linked to multiple echocardiography parameters and multiple circulating biomarkers of HF or myocardial fibrosis, indicating possible involvement of coupled excessive ventricular-arterial extracellular turnover and functional declines; and (iii) an abnormal carotid arterial strain was predictive of incident HF independent of clinical covariates which appeared to outperform myocardial systolic deformational measures with incremental value.

Various vascular studies and ultrasonic imaging modalities have been used to determine adverse vascular remodelling[5,23] or arterial stiffness;[24] these may include arterial haemodynamic indices or pulse-wave velocity measures[25] that are determined by evaluating unfavourable arterial biomechanics or physiology.[26] Despite these, few non-invasive approaches have allowed for direct assessment of vascular kinetics; these can only be achieved by more complex settings/package[27] ($\beta$-stiffness index), with limited information about dynamic arterial wall (intima-media layer) expansion. In this regard, vascular strain measurements using the speckle-tracking technique are more consistent and can be superior to conventional tools, thus providing novel insights on arterial vascular properties.[13,28] Diminished CCS was reported to be closely related to senescence,[28] hypertensive, and diabetic subjects or those with an increasing risk of atherosclerosis beyond conventional Doppler Flow information.[29–31] Outward geometric arterial remodelling by Glagov's theory has initially been proposed to be governed from physical results of flow-mediated mechanical stress on vascular wall injury.[32] In conduit arterial vasculature, this is largely regulated by endothelial nitric oxide (NO) synthesis, which may induce activation of matrix metalloproteinases, apoptosis of smooth muscle cells,[33,34] degradation/fatigue of elastin fibres, and profibrotic signalling.[35] Consequently, increased collagen deposition and cross-linking may manifest as decreased vascular distensibility.[35]

Overall, pulsatile stress generated from repetitive strain/relaxation cardiac cycle against less compliant collagen deposition within the arterial wall can be detrimental to cardiac performance, which in turn may result in diminished ejection force and deteriorated vascular deformation generation (vascular-ventricular systolic interdependence).[36] Our data demonstrated strong correlations between decreased carotid arterial strain measures and altered cardiac contractile or lusitropic properties from echocardiography, including higher E/TDI-e', worsened GLS, SRs, and SRe ($P < 0.001$, *Table 2*), with HFpEF subjects exhibiting worst carotid vascular biomechanics compared with 'healthy control' or 'high-risk' subjects without prevalent HF. The independent associations between observed vascular fragility and upregulated levels of MMP-2/PIIINP likely represent coupled LV-arterial or shared myocardial and vascular pathological processes mediated by

imbalanced extracellular matrix (ECM) remodelling, thereby declined carotid artery deformations.[8,26,28,35] Reduced capacity from stiffened conduit vasculature to buffer forward blood may in turn accelerate the rise of ventricular afterload and aggravated cardiac ECM remodelling and cardiac fibrosis leading to HFpEF.[14,37,38] As local carotid artery stiffness has been demonstrated as a strong predictor of cardiovascular events,[39] to our best knowledge, this is the first study demonstrating prognostic implications for incident HFpEF utilizing carotid artery 2D speckle-tracking method. Notably, the association of higher heart rate and reduced CCS (Supporting Information, *Table S1*) suggested accelerated arterial functional impairment by accumulated cyclic stress and diastolic phase shortening from repetitive pulsatile vascular stretch.[40] This may result in lesser time for the arterial vasculature to relax and recoil that would profoundly contribute to the pathological breakdown of elastic fibres and impact arterial remodelling.

In conclusion, our current study explored the clinical feasibility and prognostic implications of dynamic vascular functional indices using 2D speckle-tracking-based carotid deformations in a broad spectrum of cardiovascular outpatients including high-risk subjects or those with prevalent HFpEF (Stage A-C HF). CCS measures are considered a novel and non-invasive vascular imaging approach and present information regarding pulsatile arterial haemodynamic and elastic vascular wall motions; furthermore, these measures strongly correlate with advanced age, HTN, indices reflective of adverse cardiovascular events, and markers reflecting interstitial collagen turnover. Our findings highlight the complexity and coherent pathophysiological associations of HFpEF as a maladaptive LV-arterial coupling process. These findings underscore the clinical importance of adding carotid artery deformational index as an additive dimension to better characterize pathophysiology of HFpEF and serve as a surrogate marker that may outperform LV deformation in the risk stratification for HFpEF.

## Limitations

First, sample size in current study was relatively small with higher women to men ratio which limited the validity of our findings. Further, the study design did not allow comparisons or assessments of clinical treatment effects on CCS or relevant indices, as most therapeutic interventions began before data collection. Second, our current study merely explored the associations of baseline carotid artery kinetics with clinical endpoints; therefore, relations between longitudinal carotid arterial functions and clinical outcomes cannot be established. Remaining non-observed confounders may exit. Our current study had multiple hypothesis testing and more appropriate correction may be needed before accurate interpretation of current findings. As our study design aimed to

examine the prognostic implications of carotid artery deformations in a population mixed with higher clinical risk profiles or prevalent HFpEF, our findings might not be applicable and extended to subjects classified as early Stage A or B preclinical HF yet without prevalent HF (as Stage C). Further, although we observed that altered vascular kinetics are potential clinical markers and predictors of HFpEF, however, such findings may not be applicable to HFpEF pathophysiology other than senescence or HTN aetiology. Further research examining associations of altered vascular functional strains and clinical risk factors in a larger population across a broader spectrum of cardiovascular risk profiles or endpoints may be helpful to clarify these associations.

## Clinical implications

Our findings regarding the close clinical and echocardiographic correlations with vascular arterial strain measures address the possibility of using carotid artery strain as a simple and promising clinical index or a surrogate reflecting coupled ventricular-vascular functional index in clinical practices. Our study indicated that carotid vascular strain may serve as indicator for cardiac dysfunction and help in clinical grading and risk stratification of HF. This measure may also serve as an alternative treatment target in high-risk populations (e.g. HFpEF from aging or hypertensive cardiomyopathy) to develop novel therapeutic strategies, which aim for a signal-specific understanding comprehensive physiological involvement of ECM remodelling on both vascular and cardiac pathological processes, reversal of shared pathological ventricular-arterial pathologies, pathway-specific signalling (e.g. TIMPs/MMP or PIIINP axis), and decreased vascular compliance in HFpEF. As such, appropriate pathological management or downregulation/prevention of early vascular damage may theoretically prevent the insidious and vicious circle of deteriorated vascular-ventricular dysfunction, inhibiting HF development.

# Conflict of interest

None declared.

# Funding

and E-102003), and the Taiwan Foundation for Geriatric Emergency and Critical Care.

## Supporting information

Additional supporting information may be found online in the Supporting Information section at the end of the article.

**Figure S1.** Enrollment and exclusion flowchart of current study population.

**Figure S2.** Carotid vessel wall was automatically divided into six regions with verification of adequate tracking for all six segments for CCS (A), with CRS and CRD presented (B and C).

**Figure S3.** Histogram of carotid arterial deformation indices of current study.

**Figure S4.** Comparisons of carotid arterial deformation indices between baseline Non-HFpEF and HFpEF of current study.

**Figure S5.** Sex-stratified analysis on associations of CCS with biomarkers and echocardiography information.

**Table S1.** Associations of baseline characteristics with CCS, CCRS, CRS, and CRD.

**Table S2.** Associations of carotid arterial deformation with biomarkers and echocardiography information.

**Table S3.** NRI table showing incremental values of CCS over cardiac contractility indices (GLS) for HF event.

## References

1. Kitzman DW, Gardin JM, Gottdiener JS, Arnold A, Boineau R, Aurigemma G, Marino EK, Lyles M, Cushman M, Enright PL; Cardiovascular Health Study Research Group. Importance of heart failure with preserved systolic function in patients ≥65 years of age. CHS Research Group. Cardiovascular Health Study. *Am J Cardiol* 2001; **87**:413–419.
2. Ziaeian B, Fonarow GC. Epidemiology and aetiology of heart failure. *Nat Rev Cardiol* 2016; **13**: 368–378.
3. Altara R, Giordano M, Nordén ES, Cataliotti A, Kurdi M, Bajestani SN, Booz GW. Targeting obesity and diabetes to treat heart failure with preserved ejection fraction. *Front Endocrinol (Lausanne)* 2017; **8**: 160.
4. Lam CS, Roger VL, Rodeheffer RJ, Bursi F, Borlaug BA, Ommen SR, Kass DA, Redfield MM. Cardiac structure and ventricular-vascular function in persons with heart failure and preserved ejection fraction from Olmsted County, Minnesota. *Circulation* 2007; **115**: 1982–1990.
5. Fernandes VR, Polak JF, Cheng S, Rosen BD, Carvalho B, Nasir K, McClelland R, Hundley G, Pearson G, O'Leary DH, Bluemke DA, Lima JA. Arterial stiffness is associated with regional ventricular systolic and diastolic dysfunction: the multi-ethnic study of atherosclerosis. *Arterioscler Thromb Vasc Biol* 2008; **28**: 194–201.
6. Gardin JM, Arnold AM, Polak J, Jackson S, Smith V, Gottdiener J. Usefulness of aortic root dimension in persons > or = 65 years of age in predicting heart failure, stroke, cardiovascular mortality, all-cause mortality and acute myocardial infarction (from the cardiovascular health study). *Am J Cardiol* 2006; **97**: 270–275.
7. Borlaug BA, Lam CS, Roger VL, Rodeheffer RJ, Redfield MM. Contractility and ventricular systolic stiffening in

hypertensive heart disease insights into the pathogenesis of heart failure with preserved ejection fraction. *J Am Coll Cardiol* 2009; **54**: 410–418.
8. Chen CH, Nakayama M, Nevo E, Fetics BJ, Maughan WL, Kass DA. Coupled systolic-ventricular and vascular stiffening with age: implications for pressure regulation and cardiac reserve in the elderly. *J Am Coll Cardiol* 1998; **32**: 1221–1227.
9. Leite-Moreira AF, Correia-Pinto J, Gillebert TC. Afterload induced changes in myocardial relaxation: a mechanism for diastolic dysfunction. *Cardiovasc Res* 1999; **43**: 344–353.
10. Kawaguchi M, Hay I, Fetics B, Kass DA. Combined ventricular systolic and arterial stiffening in patients with heart failure and preserved ejection fraction: implications for systolic and diastolic reserve limitations. *Circulation* 2003; **107**: 714–720.
11. Kass DA. Ventricular arterial stiffening: integrating the pathophysiology. *Hypertension* 2005; **46**: 185–193.
12. Borlaug BA, Olson TP, Lam CS, Flood KS, Lerman A, Johnson BD, Redfield MM. Global cardiovascular reserve dysfunction in heart failure with preserved ejection fraction. *J Am Coll Cardiol* 2010; **56**: 845–854.
13. Bjällmark A, Lind B, Peolsson M, Shahgaldi K, Brodin LA, Nowak J. Ultrasonographic strain imaging is superior to conventional non-invasive measures of vascular stiffness in the detection of age-dependent differences in the mechanical properties of the common carotid artery. *Eur J Echocardiogr* 2010; **11**: 630–636.
14. Geyer H, Caracciolo G, Abe H, Wilansky S, Carerj S, Gentile F, Nesser HJ, Khandheria B, Narula J, Sengupta PP. Assessment of myocardial mechanics using speckle tracking

echocardiography: fundamentals and clinical applications. *J Am Soc Echocardiogr* 2010; **23**: 351–369.
15. Podgórski M, Grzelak P, Kaczmarska M, Polguj M, Łukaszewski M, Stefańczyk L. Feasibility of two-dimensional speckle tracking in evaluation of arterial stiffness: comparison with pulse wave velocity and conventional sonographic markers of atherosclerosis. *Vascular* 2018; **26**: 63–69.
16. Becker M, Bilke E, Kuhl H, Katoh M, Kramann R, Franke A, Bucker A, Hanrath P, Hoffmann R. Analysis of myocardial deformation based on pixel tracking in two dimensional echocardiographic images enables quantitative assessment of regional left ventricular function. *Heart* 2006; **92**: 1102–1108.
17. Patton DM, Li T, Hétu MF, Day AG, Preece E, Matangi MF, Johri AM. Speckle tracking carotid artery circumferential strain is a marker of arterial sclerosis but not coronary atheroma. *J Clin Ultrasound* 2018; **46**: 575–581.
18. Liao ZY, Peng MC, Yun CH, Lai YH, Po HL, Hou CJ, Kuo JY, Hung CL, Wu YJ, Bulwer BE, Yeh HI, Tsai CH. Relation of carotid artery diameter with cardiac geometry and mechanics in heart failure with preserved ejection fraction. *J Am Heart Assoc* 2012; **1**: e003053.
19. Larsson M, Heyde B, Kremer F, Brodin LÅ, D'hooge J. Ultrasound speckle tracking for radial, longitudinal and circumferential strain estimation of the carotid artery—an in vitro validation via sonomicrometry using clinical and high-frequency ultrasound. *Ultrasonics* 2015; **56**: 399–408.
20. Saito M, Okayama H, Inoue K, Yoshii T, Hiasa G, Sumimoto T, Nishimura K, Ogimoto A, Higaki J. Carotid arterial circumferential strain by two-dimensional speckle tracking: a novel parameter of

arterial elasticity. *Hypertens Res* 2012; **35**: 897–902.

21. Yoon JH, Cho IJ, Chang HJ, Sung JM, Lee J, Ryoo H, Shim CY, Hong GR, Chung N. The value of elastic modulus index as a novel surrogate marker for cardiovascular risk stratification by dimensional speckle-tracking carotid ultrasonography. *J Cardiovasc Ultrasound* 2016; **24**: 215–222.

22. Yang JW, Cho KI, Kim JH, Kim SY, Kim CS, You GI, Lee JY, Choi SY, Lee SW, Kim HS, Heo JH, Cha TJ, Lee JW. Wall shear stress in hypertensive patients is associated with carotid vascular deformation assessed by speckle tracking strain imaging. *J Clin Hypertens* 2014; **20**: 10.

23. Cavalcante JL, Lima JA, Redheuil A, Al-Mallah MH. Aortic stiffness: current understanding and future directions. *J Am Coll Cardiol* 2011; **57**: 1511–1522.

24. Vlachopoulos C, Aznaouridis K, Stefanadis C. Prediction of cardiovascular events and all-cause mortality with arterial stiffness: a systematic review and meta-analysis. *J Am Coll Cardiol* 2010; **55**: 1318–1327.

25. Yamashina A, Tomiyama H, Takeda K, Tsuda H, Arai T, Hirose K, Koji Y, Hori S, Yamamoto Y. Validity, reproducibility, and clinical significance of noninvasive brachial-ankle pulse wave velocity measurement. *Hypertens Res* 2002; **25**: 359–364.

26. Lakatta EG, Levy D. Arterial and cardiac aging: major shareholders in cardiovascular disease enterprises: part I: aging arteries: a "set up" for vascular disease. *Circulation* 2003; **107**: 139–146.

27. Hirai T, Sasayama S, Kawasaki T, Yagi S. Stiffness of systemic arteries in patients with myocardial infarction. A noninvasive method to predict severity of coronary atherosclerosis. *Circulation* 1989; **80**: 78–86.

28. Rosenberg AJ, Lane-Cordova AD, Wee SO, White DW, Hilgenkamp TIM, Fernhall B, Baynard T. Healthy aging and carotid performance: strain measures and β-stiffness index. *Hypertens Res* 2018; **41**: 748–755.

29. Park HE, Cho GY, Kim HK, Kim YJ, Sohn DW. Validation of circumferential carotid artery strain as a screening tool for subclinical atherosclerosis. *J Atheroscler Thromb* 2012; **19**: 349–356.

30. Yang EY, Brunner G, Dokainish H, Hartley CJ, Taffet G, Lakkis N, Taylor AA, Misra A, McCulloch ML, Morrisett JD, Virani SS, Ballantyne CM, Nagueh SF, Nambi V. Application of speckle-tracking in the evaluation of carotid artery function in subjects with hypertension and diabetes. *J Am Soc Echocardiogr* 2013; **26**: 901–909.e1.

31. Yang EY, Dokainish H, Virani SS, Misra A, Pritchett AM, Lakkis N, Brunner G, Bobek J, McCulloch ML, Hartley CJ, Ballantyne CM, Nagueh SF, Nambi V. Segmental analysis of carotid arterial strain using speckle-tracking. *J Am Soc Echocardiogr* 2011; **24**: 1276–1284.e5.

32. Korshunov VA, Schwartz SM, Berk BC. Vascular remodeling: hemodynamic and biochemical mechanisms underlying Glagov's phenomenon. *Arterioscler Thromb Vasc Biol* 2007; **27**: 1722–1728.

33. Tronc F, Wassef M, Esposito B, Henrion D, Glagov S, Tedgui A. Role of NO in flow-induced remodeling of the rabbit common carotid artery. *Arterioscler Thromb Vasc Biol* 1996; **16**: 1256–1262.

34. Ward MR, Pasterkamp G, Yeung AC, Borst C. Arterial remodeling. Mechanisms and clinical implications. *Circulation* 2000; **102**: 1186–1191.

35. Redfield MM, Jacobsen SJ, Borlaug BA, Rodeheffer RJ, Kass DA. Age- and gender-related ventricular-vascular stiffening: a community-based study. *Circulation* 2005; **112**: 2254–2262.

36. López B, Ravassa S, González A, Zubillaga E, Bonavila C, Bergés M, Echegaray K, Beaumont J, Moreno MU, San José G, Larman M, Querejeta R, Díez J. Myocardial collagen cross-linking is associated with heart failure hospitalization in patients with hypertensive heart failure. *J Am Coll Cardiol* 2016; **67**: 251–260.

37. Kim SA, Park SM, Kim MN, Kim YH, Cho DH, Ahn CM, Hong SJ, Lim DS, Shim WJ. The relationship between mechanical properties of carotid artery and coronary artery disease. *Eur Heart J Cardiovasc Imaging* 2012; **13**: 568–573.

38. Martos R, Baugh J, Ledwidge M, O'Loughlin C, Murphy NF, Conlon C, Patle A, Donnelly SC, McDonald K. Diagnosis of heart failure with preserved ejection fraction: improved accuracy with the use of markers of collagen turnover. *Eur J Heart Fail* 2009; **11**: 191–197.

39. van Sloten TT, Schram MT, van den Hurk K, Dekker JM, Nijpels G, Henry RM, Stehouwer CD. Local stiffness of the carotid and femoral artery is associated with incident cardiovascular events and all-cause mortality: the Hoorn study. *J Am Coll Cardiol* 2014; **63**: 1739–1747.

40. Giannattasio C, Vincenti A, Failla M, Capra A, Ciro A, De Ceglia S, Gentile G, Brambilla R, Mancia G. Effects of heart rate changes on arterial distensibility in humans. *Hypertension* 2003; **42**: 253–256.